

RAPID COMMUNICATION

Synthesis of isotopically controlled metal-catalyzed silicon nanowires

Oussama Moutanabbir*, Stephan Senz, Zhang Zhang, Ulrich Gösele

Max Planck Institute of Microstructure Physics, Weinberg 2, D 06120 Halle (Saale), Germany

Received 22 July 2009; received in revised form 15 August 2009; accepted 20 August 2009

Available online 9 September 2009

KEYWORDS

Nanowires;
Semiconductor;
Stable isotopes;
Metal-catalyzed
growth;
Epitaxy;
Chemical vapor
deposition

Summary This work demonstrates the growth of isotopically controlled silicon nanowires by the vapor–liquid–solid mechanism. The growth is accomplished by using silane precursors $^{28}\text{SiH}_4$, $^{29}\text{SiH}_4$, and $^{30}\text{SiH}_4$ synthesized from SiF_4 isotopically enriched in a centrifugal setup. We grew monoisotopic ^{28}Si , ^{29}Si , and ^{30}Si nanowires with isotopic purity of 99.99%, 99.9%, and 99.9%, respectively. The properties of Si–Si LO phonons of individual monoisotopic nanowires attached to silicon substrate are presented. The control of the isotopic composition of silicon on the nanoscale creates new opportunities to improve our understanding of the fundamental properties of nanowire-based devices.

© 2009 Elsevier Ltd. All rights reserved.

Silicon nanowires (SiNWs) have received a great deal of attention as powerful nanotechnological building blocks with a potential impact on various fields such as nano-electronics [1,2], clean energy [3,5], biosensing [6], and quantum information [7] to name just a few. Among all synthesis methods, the vapor–liquid–solid (VLS) process appears to be the most successful in generating high densities of single crystalline nanowires [8]. In this process, the growth of nanowires is accomplished via a liquid metal cluster which acts catalytically as the energetically favored site for vapor-phase reactant absorption and when saturated, the nucleation site for crystallization and one-dimensional growth [8,9]. Gold (Au) is the most frequently used catalyst for the growth of SiNWs. Tiny Au–Si alloy droplets can form by deposition of a thin Au layer on Si and sub-

sequent annealing above the eutectic temperature of the Au–Si system ($\sim 363^\circ\text{C}$). These nanodroplets absorb efficiently Si from the gaseous precursor. The supersaturation of these AuSi alloy nanodroplets triggers the nucleation of one-dimensional nanocrystals—the nanowires. The diameter of the SiNW is determined by the size of the initial droplet, which can be influenced by the substrate temperature and the thickness of the initial Au layer. The growth can also be achieved below the eutectic temperature with solid catalyst particles [10,11]. Under these conditions, the growth occurs via the vapor–solid–solid mechanism.

To date, natural silicon (^{nat}Si) is used exclusively in the growth of SiNWs. ^{nat}Si is composed of three stable isotopes: ^{28}Si , ^{29}Si , and ^{30}Si with abundances of 92.23%, 4.67%, and 3.10%, respectively. These abundances are a consequence of the nucleosynthesis that led to the formation of the elements making up the matter in the universe. In general, several physical properties of semiconductor crystals can be significantly influenced by their isotopic composition [12–18]. This is due to the following differences among the

* Corresponding author. Tel.: +49 345 5582912;

fax: +49 345 5511223.

E-mail address: moutanab@mpi-halle.mpg.de (O. Moutanabbir).

Table 1 Isotopic content of the three varieties of monoisotopic monosilane used in this study. The shaded cells correspond to the isotopic purity of different precursors.

	Isotopic composition [%]		
	$^{28}\text{SiH}_4$	$^{29}\text{SiH}_4$	$^{30}\text{SiH}_4$
Precursors			
$^{28}\text{SiH}_4$	99.99440 ± 0.00272	0.00526 ± 0.00271	0.00034 ± 0.00012
$^{29}\text{SiH}_4$	0.041 ± 0.010	99.909 ± 0.019	0.050 ± 0.015
$^{30}\text{SiH}_4$	0.0140 ± 0.0050	0.042 ± 0.007	99.944 ± 0.010

isotopes: (1) the atomic mass; (2) the nuclear spin; and (3) the nuclear transmutation induced by the capture of a thermal neutron. In bulk Si, the physical properties can change drastically depending on the relative proportions of ^{28}Si , ^{29}Si , and ^{30}Si . Indeed, the small variation in the atomic mass induces a change in phonon energies, band structure, and lattice constant [16,17]. Large isotopic effects were observed around the thermal conductivity maximum [17]. More subtle nuclear spin-related isotopic effects (only ^{29}Si has a nuclear spin of 1/2) have been exploited to investigate Si-based quantum information devices [19,20]. By capturing a thermal neutron, ^{28}Si , ^{29}Si , and ^{30}Si transmute into ^{29}Si , ^{30}Si , and ^{31}Si , respectively. Interestingly, ^{31}Si is unstable and decays by β^- emission leading to the formation of ^{31}P which is a *n*-type dopant in Si. Highly uniform doping can be achieved via this process—commonly known as neutron transmutation doping (NTD) [21]. Combining the advances in nanofabrication with what can be achieved by stable and enriched isotopes provides a rich playground to explore the origin of some basic size-related properties in nanoscale structures. In this paper, we report the first demonstration of the growth of isotopically controlled metal-catalyzed SiNWs by using isotopically purified precursors. This increase of the complexity by the controlled manipulation of the isotopic composition during the growth creates new opportunities to enhance our theoretical understanding of the fundamental properties of SiNWs and their potential technological applications.

Stable and enriched isotopes play critical roles in a variety of technological applications and have many scientific uses in the fields of experimental physics, geology, biology, pharmacology, and environmental and materials sciences [22]. The isotope separation can be achieved by electromagnetic methods, laser excitation, thermal diffusion, chemical exchanges, and gas centrifugation [23–25]. When the element to be separated can be prepared as a gaseous compound, the technique of choice for isotope purification is the centrifuge-based technology (Zippe-centrifuge) [25]. Si is isotopically enriched by using tetrafluoride silicon (SiF_4). $^{28}\text{SiF}_4$, $^{29}\text{SiF}_4$, and $^{30}\text{SiF}_4$ with high isotopic purity are produced in a centrifugal setup. Monoisotopic silane precursors used in this work were synthesized from $^{28}\text{SiF}_4$, $^{29}\text{SiF}_4$, and $^{30}\text{SiF}_4$ and calcium hydride following the reaction [26]: $\text{SiF}_4 + 2\text{CaH}_2 \rightarrow \text{SiH}_4 + \text{CaF}_2$. The monoisotopic monosilane precursors $^{28}\text{SiH}_4$, $^{29}\text{SiH}_4$, and $^{30}\text{SiH}_4$ have an isotopic purity of (99.994 ± 0.003) %, (99.909 ± 0.019) %, and (99.944 ± 0.010) %, respectively. The enrichment and purification were performed at the Institute of Chemistry of High Purity Substances of the Russian Academy of Sciences

(Nizhny Novgorod, Russia). The exact isotopic content of each precursor is given in Table 1.

In this work, SiNW growth experiments were carried out in an ultrahigh vacuum chemical vapor deposition reactor (UHV-CVD) with a background pressure of $<1.0 \times 10^{-10}$ mbar. *N*-type phosphorous-doped $^{29}\text{Si}(111)$ wafers were used as substrates in our experiments. The substrates surface was conditioned by a standard wet chemical cleaning followed by a dip in 2% hydrofluoric acid to hydrogen-passivate the surface. The wafers were immediately transferred into the UHV-CVD reactor. A 1 nm-thick Au film was then deposited onto the substrate by a thermal evaporation source. Immediately after Au deposition, the substrate was annealed for 20 min at 650 °C. During annealing the Au film breaks up into Au–Si nanodroplets. The growth of the isotopically controlled SiNWs was accomplished by introducing the enriched silane precursors: $^{28}\text{SiH}_4$, $^{29}\text{SiH}_4$, and $^{30}\text{SiH}_4$. The partial pressure of the silane was kept below 0.15 mbar. The grown isotopically controlled SiNWs were characterized using scanning electron microscope (FEI Dualbeam Nanolab 600) and visible confocal Raman scattering spectroscopy. Micro-Raman analysis was performed in backscattering geometry by a LabRam HR800 UV spectrometer with a 488 nm Ar ion laser. A 100× objective was used to focus the laser beam to a spot of $\sim 1 \mu\text{m}$ in diameter. The backscattered Raman light is diffracted by a 2400 g/mm grating and detected by a charge-coupled device camera. The spectral distance between adjacent channels is $\sim 0.4 \text{ cm}^{-1}$. This setup enables the determination of Raman shift with an accuracy of 0.2 cm^{-1} . The Au caps were removed by etching in a KI/I_2 mixture before Raman measurements. A CCD camera was used to focus the laser beam on a single SiNW vertically aligned on the $^{29}\text{Si}(111)$ substrate. Samples with a very low SiNW density were used in the Raman investigations.

During growth, the composition of the silane was monitored *in situ* by a mass spectrometer. Fig. 1 displays the spectra of different precursors used in the growth. For comparison, the spectrum of $^{29}\text{SiH}_4$ is also shown. The spectra of the monoisotopic silanes are characterized by four main Si-related peaks attributed to Si, SiH, SiH₂, and SiH₃ monoisotopic ions. Due to the mixing of the three isotopes, two additional peaks are observed for $^{29}\text{SiH}_4$. Depending on the growth parameters, the diameter of the grown nanowires ranges from a few nanometers to a few hundred nanometers while the length can reach several micrometers. Fig. 2 displays a selected set of scanning electron microscopy (SEM) images of $^{28}\text{SiNWs}$, $^{29}\text{SiNWs}$, and $^{30}\text{SiNWs}$ vertically aligned on $^{29}\text{Si}(111)$. The growth rates of different monoisotopic SiNWs are expected to vary within

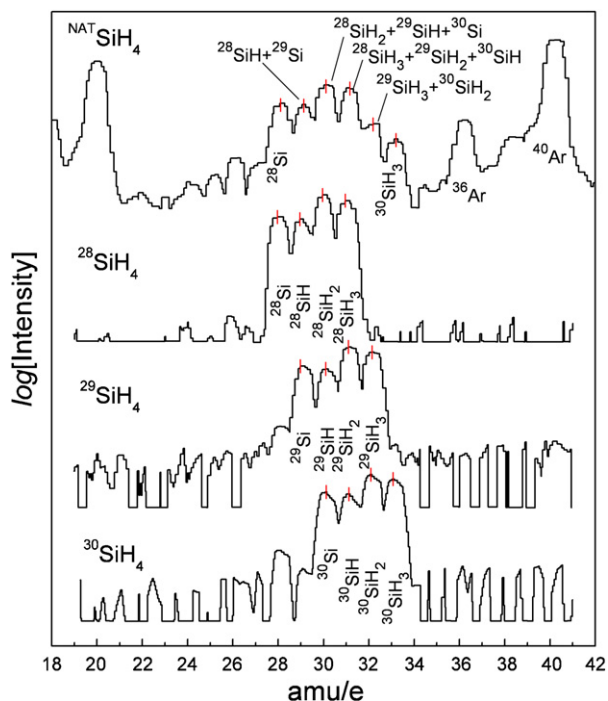


Figure 1 *In situ* mass spectrometer spectra of different precursors. Note that the spectra of the monoisotopic sources are dominated by four peaks: Si, SiH, SiH₂, and SiH₃. The small peaks at 28 and 29 in ²⁹SiH₄ and ³⁰SiH₄ spectra originate from ²⁸Si “impurities”. ^{NAT}SiH₄ spectrum shows additional peaks due to the isotopic mixing. The ^{NAT}SiH₄ is diluted with Ar. Note the vertical logarithmic scale.

~1.8% due to the slight influence of the atomic mass on the transport of Si atoms within the catalyst nanodroplets [27]. However, this very small variation in the growth rate cannot be responsible of the observed differences in the morphological properties of the grown SiNWs (Fig. 2), which we believe comes simply from the fluctuations in the silane flux during the growth experiments with different precursors.

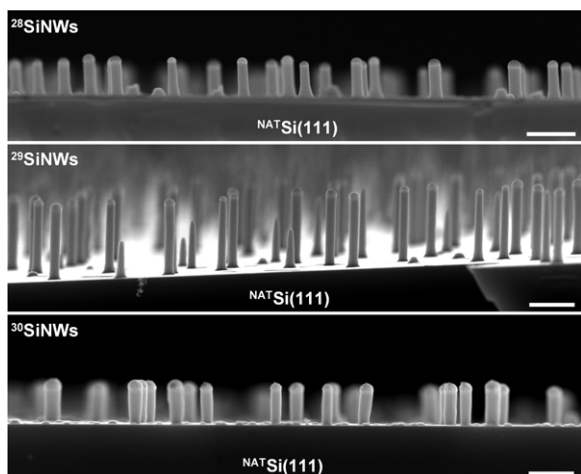


Figure 2 Scanning electron microscopy image of isotopically purified SiNWs: (a) ²⁹SiNWs; (b) ²⁸SiNWs; and (c) ³⁰SiNWs grown at 600 °C. The average growth rates are 21.15, 19.00, and 18.12 nm/min for ²⁸SiNWs, ²⁹SiNWs, and ³⁰SiNWs, respectively. The scale bar denotes 1 μm.

The vibrational properties of the as-grown monoisotopic SiNWs are investigated next. The phonons in SiNWs have been the subject of extensive investigations because they contain a wealth of information on the structural and electro-optical characteristics [28]. However, it is worth noting that all the experimental studies reported so far required the growth on a foreign substrate or the removal of SiNWs from the original substrate and their transfer onto a foreign substrate to eliminate the background arising from the underlying Si. The nature of the contact with the host substrate was found to affect strongly the vibrational properties of SiNWs and can lead to inaccurate interpretations of Raman data [28]. Conspicuously absent in the literature is the investigation of the phonon properties of a single as-grown SiNW attached to a Si substrate in spite of the crucial and precise information it could provide concerning the structural properties and also the nature of the nanowire-substrate thermal contact. Here we demonstrate that the use of the enriched isotopes enables the investigation of the phonon properties of SiNW-on-Si system. Indeed, a simple harmonic analysis within the virtual crystal approximation predicts that the frequency ω of a given phonon should vary with the average atomic mass m : $\omega \propto m^{-1/2}$. The average atomic mass is given by $m = \sum_i \theta_i \times m_i$, where θ_i and m_i are the content and atomic mass of each Si isotope, respectively. Therefore, the Si–Si LO phonon of SiNWs with larger average atomic mass than ^{NAT}Si can be detected at lower wavenumbers without the need to remove the nanowires

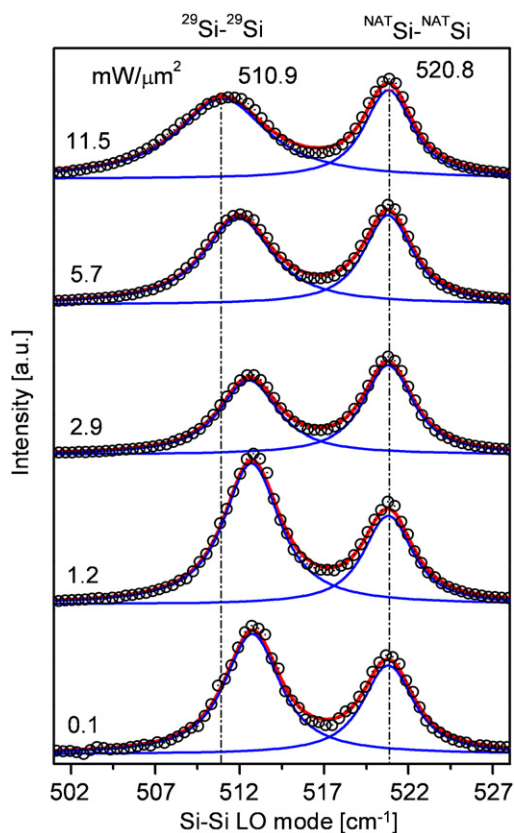


Figure 3 Si–Si Raman spectra of ²⁹SiNWs attached to ^{NAT}Si(111) substrate as a function of the 488 nm excitation power. The solid lines presents Voigt-function fits.

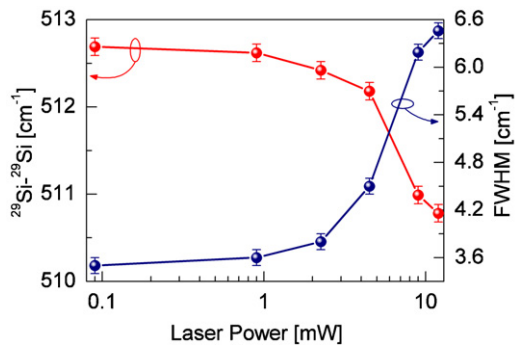


Figure 4 The evolution of Raman shift ω and FWHM of $^{29}\text{Si}-^{29}\text{Si}$ mode of $^{29}\text{SiNW}$ as a function of laser power.

from the Si substrate as shown in Fig. 3. This figure displays a selected set of Raman spectra of $^{29}\text{SiNW}$ with a diameter of ~ 100 nm and a length of ~ 1.5 μm vertically aligned on $^{\text{NAT}}\text{Si}(111)$ substrate. The spectra were recorded under different laser power densities. Two Raman peaks are detected at ~ 511 and 520.8 cm^{-1} corresponding to the LO phonons in $^{29}\text{SiNW}$ ($^{29}\text{Si}-^{29}\text{Si}$) and in the underlying $^{\text{NAT}}\text{Si}$ substrate, respectively. It is noticeable that by increasing the laser power the $^{29}\text{Si}-^{29}\text{Si}$ Raman mode broadens and shifts to lower wavenumbers. In contrast, the Si-Si Raman peak of the underlying $^{\text{NAT}}\text{Si}(111)$ substrate remains insensitive to the change in the laser power. Fig. 4 shows the evolution of ω and the full width at half maximum (FWHM) in the laser power range of 0.09–12 mW. We note that ω increases from 510.8 cm^{-1} at the highest power to 512.7 cm^{-1} at the lowest power. In parallel, FWHM decreases from 6.5 to 3.5 cm^{-1} . These observations demonstrate that, due to the reduced thermal conductivity [29], the local temperature of $^{29}\text{SiNW}$ increases significantly when exposed to the laser beam indicative of a poor thermal anchorage and/or limited heat spreading within the $^{29}\text{SiNW}/\text{bulk } ^{\text{NAT}}\text{Si}$ system. Note that the investigated SiNWs are too large to exhibit any confinement-related asymmetric broadening. A symmetric Raman line is detected in the absence of the laser heating below 0.1 $\text{mW}/\mu\text{m}^2$ with a FWHM of 3.5 cm^{-1} comparable to the FWHM of bulk Si mode (~ 3.3 cm^{-1}) in this experiment indicating a high crystalline quality of the grown SiNWs.

Fig. 5 shows Raman spectra of the three varieties of monoisotopic nanowires attached to $^{\text{NAT}}\text{Si}(111)$ substrates recorded at low laser power density. For $^{29}\text{SiNW}$ and $^{30}\text{SiNW}$ distinct peaks are detected at 512.69 and 504.96 cm^{-1} , respectively. No clear peak is observed for $^{28}\text{SiNW}$ s due to the overlap with the strong signal from the underlying $^{\text{NAT}}\text{Si}(111)$ substrate. From the harmonic approximation described above, the expected frequency of the Si-Si Raman peak of the isotopically controlled SiNWs can be expressed as: $\omega_{\text{NW}}^{\text{isotope}} = \omega_{\text{NAT}} \times \sqrt{m_{\text{NAT}}/m_{\text{isotope}}}$, where ω_{NAT} is the Si-Si Raman frequency of $^{\text{NAT}}\text{Si}$ (underlying substrate), and m_{NAT} and m_{isotope} are the average atomic masses of $^{\text{NAT}}\text{Si}$ and the enriched isotope used in the growth, respectively. This is a valid approximation for systems with very low mass disorder. For deliberately isotopically mixed systems, the scaling law is modified by anharmonic and mass disorder-induced contributions (see Ref. [16] and references therein). $m_{\text{NAT}} = 28.08553$ amu. m_{isotope} can be estimated from the isotopic content and atomic mass of each iso-

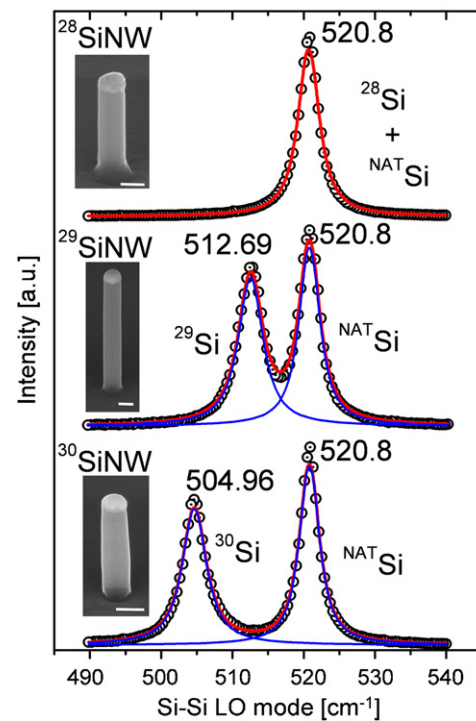


Figure 5 Raman scattering spectra of monoisotopic SiNWs vertically aligned on $^{\text{NAT}}\text{Si}(111)$ substrates. The spectra were recorded using a 488 nm Ar^+ laser with a power of ~ 10 μW to avoid local heating effects. Inset: SEM images of the corresponding monoisotopic nanowires. The scale bar denotes 100 nm.

tope ($m_{^{28}\text{Si}} = 27.9769265325$ amu, $m_{^{29}\text{Si}} = 28.976494700$ amu, and $m_{^{30}\text{Si}} = 29.97377017$ amu). From Table 1, we estimate the frequencies of the Si-Si Raman peak of the monoisotopic SiNWs: $\omega_{\text{NW}}^{^{28}\text{Si}} = 520.81$ cm^{-1} , $\omega_{\text{NW}}^{^{29}\text{Si}} = 512.73$ cm^{-1} , and $\omega_{\text{NW}}^{^{30}\text{Si}} = 504.14$ cm^{-1} . For $^{29}\text{SiNW}$, the calculated frequency (512.73 cm^{-1}) is practically identical to the experimental value (512.69 cm^{-1}) confirming the expected isotopic purity of $\sim 99.9\%$. ~ 0.8 cm^{-1} difference is found between the calculated and experimental frequencies of Si-Si LO phonon in $^{30}\text{SiNW}$.

The control of the isotopic content during the growth of SiNWs provides a rich playground to investigate systematically SiNW-based systems in a wide range of applications. A number of isotope effects are related to the change in the properties of phonons with atomic mass. The most drastic phonon-related isotope effect is found for thermal conductivity. Pomeranchuk has demonstrated the role of isotope ‘‘impurities’’ as phonon scatterers with a resulting influence on the thermal conductivity [30]. More specifically, the maximum thermal conductivity was found to be strongly affected by the isotopic composition. Besides the change in the average atomic mass, the isotopic substitution creates ‘‘perfect’’ point defects, producing mass disorder that influences phonon scattering. Klemens derived for such scattering a mean free path $L_{\text{isotope}} \sim g \times T^4$, where g presents the isotopic mass variance [31]: $g = \left(\sum \theta_i \times m_i^2 - \left(\sum \theta_i \times m_i \right)^2 \right) / \left(\sum \theta_i \times m_i \right)^2$. Therefore, assuming a similar phonon behavior as in bulk, it is possible to tune the thermal conductivity of SiNWs by a

controlled manipulation of the isotopic content during the VLS growth. High isotopic purity corresponds to a small value of g , whereas high isotopic disorder by the deliberate mixing of the isotopes gives higher g . Exploring this effect in SiNWs will provide greater insights into the basic mechanisms of thermal conductance and heat transport in nanoscale Si structures. Understanding these fundamental aspects is vital for SiNW-based thermoelectric devices [3,4].

By alternating different monoisotopic silanes during the VLS growth, more nanowire complex structures could be obtained. The distribution of the isotope clusters can be controlled either axially or radially. These isotopic heterostructures can hardly be achieved using other nanofabrication processes. Radial and axial isotopic multilayer SiNWs are model systems to test different theories of phonon dispersion in SiNWs and to highlight more subtle mechanisms in the process of phonon scattering. These isotopic superlattice nanowires also provide an efficient approach to achieve ultralow thermal conductivity values which can improve thermoelectric performance and prevent the back-flow of heat as suggested by recent theoretical calculations [32]. Moreover, axial multilayers with ^{30}Si clusters embedded in ^{28}Si SiNWs can be used for a precise introduction of ^{31}P dopant atoms by NTD [21]. The spatial control of ^{31}P atoms in nuclear spin-free Si is a prerequisite for the implementation of electron-spin Si-based quantum computing [33]. In addition to the precise control of P donors, implementing the electron-spin quantum computer requires a high enrichment of zero-nuclear spin Si (i.e., depleted from ^{29}Si impurities) as the nuclear spin of ^{29}Si affects the electron-spin coherence time. While being undesirable in electron-spin-based quantum computer, ^{29}Si nuclei were suggested as building blocks for another solid-state quantum information processor. Metal-catalyzed growth is a method by which ^{29}Si clusters can be precisely placed within a nuclear spin-free ^{28}Si SiNW thereby leading to the realization, at least from a materials standpoint, of all-silicon nuclear magnetic resonance quantum devices [20]. Finally, it is important to note that, due to the high Si solubility in SiAu alloy droplets, using Au as a catalyst can produce isotopic heterostructures with a smeared out interfaces. The material mixing issue can be overcome by using Al as a catalyst. With a Si solubility of $\sim 2\%$ at the usual growth temperatures, Al-synthesized nanowire heterostructures are expected to display sharp interfaces [10].

In summary, we have demonstrated the growth of isotopically controlled silicon nanowires by the VLS mechanism. The growth was accomplished by using isotopically enriched silane precursors $^{28}\text{SiH}_4$, $^{29}\text{SiH}_4$, and $^{30}\text{SiH}_4$ with isotopic purity of 99.99%, 99.9%, and 99.9%, respectively. The properties of Si-Si LO phonon of individual monoisotopic nanowire attached to silicon substrate were presented. This artificial manipulation of the isotopic composition of Si on the nanoscale creates new opportunities to explore fundamental science and improve our understanding of the physical properties of SiNWs including the isotopic nanowire heterostructures.

References

- [1] K.D. Ferry, *Science* 319 (2008) 579.
- [2] Y. Cui, C.M. Lieber, *Science* 291 (2002) 851.
- [3] A.I. Hochbaum, et al., *Nature* 451 (2007) 163.
- [4] A.I. Boukai, et al., *Nature* 451 (2007) 168.
- [5] B. Tian, et al., *Nature* 449 (2007) 885.
- [6] Z. Li, et al., *Nano Lett.* 4 (2004) 245.
- [7] Y. Hu, et al., *Nat. Nanotech.* 2 (2007) 622.
- [8] R.S. Wagner, W.C. Ellis, *Appl. Phys. Lett.* 4 (1964) 89.
- [9] B. Kim, et al., *Science* 322 (2008) 1070.
- [10] Y. Wang, V. Schmidt, S. Senz, U. Gösele, *Nat. Nanotech.* 1 (2006) 186.
- [11] S. Kodambaka, et al., *Science* 316 (2007) 729.
- [12] A.A. Berezin, *J. Phys. Chem. Solids* 50 (1989) 5.
- [13] E.E. Haller, *J. Appl. Phys.* 77 (1995) 2857.
- [14] K. Itoh, *J. Mater. Res.* 8 (1993) 1341.
- [15] M. Cardona, in: R. Helbig (Ed.), *Advances in Solid State Physics*, Vieweg, Braunschweig, 1995.
- [16] M. Cardona, M.L. Thewalt, *Rev. Mod. Phys.* 77 (2005) 1173.
- [17] J.W. Ager III, E.E. Haller, *Physica Status Solidi A* 203 (2006) 3550; V.G. Plekhanov, *Prog. Mater. Sci.* 51 (2006) 287.
- [18] E.E. Haller, *MRS Bull.* 31 (2006) 547.
- [19] T.D. Ladd, et al., *Phys. Rev. Lett.* 89 (2002) 017901.
- [20] K.M. Itoh, *Solid State Commun.* 133 (2005) 747.
- [21] J. Messe (Ed.), *Neutron Transmutation Doping in Semiconductors*, Plenum Press, New York, 1979.
- [22] See for e.g., the report of the workshop *on the Nation's Need for Isotopes: Present and Future*, Rockyville, Maryland, August 5–7, 2008. The report is available online: http://www.sc.doe.gov/henp/np/program/docs/Workshop%20Report_final.pdf.
- [23] L.O. Love, *Science* 182 (1972) 343.
- [24] S. Villani, *Isotope Separation*, American Nuclear Society, Hinsdale, IL, 1976.
- [25] D. Olander, *Sci. Am.* 239 (1978) 37.
- [26] G.G. Devyatikh, et al., *Dokl. Chem.* 376 (2001) 47.
- [27] The growth rate (v) can be expressed by: $v = \Delta C D / \rho r$, where ΔC is the Si concentration gradient across the nanodroplet, D the diffusion constant of Si, ρ the atomic density of Si, and r the radius of the nanodroplets. Since ^{28}Si , ^{29}Si , and ^{30}Si are chemically identical, only D depends on the atomic mass. The ratio of the diffusion coefficients of two isotopes i and j in a liquid system should vary with the average atomic mass [34]: $D_i/D_j \propto (m_j/m_i)^{1/2}$. The same relationship should govern the ratio of the growth rates (i.e., $v_i/v_j \propto (m_j/m_i)^{1/2}$).
- [28] For a recent review see: K.W. Adu, H.R. Gutierrez, P.C. Eklund, in: V. Kumar (Ed.), *Nanosilicon*, Elsevier, 2008, pp. 258–288.
- [29] D. Li, et al., *Appl. Phys. Lett.* 83 (2003) 2934.
- [30] I. Pomeranchuk, *J. Phys. (Moscow)* 5 (1942) 237.
- [31] P.G. Klemens, *Proc. Phys. Soc. Lond. A* 68 (1955) 1113.
- [32] N. Yang, G. Zhang, B. Li, *Nano Lett.* 8 (2008) 276.
- [33] B.E. Kane, *Nature* 393 (1998) 1331.
- [34] L.W. Barr, M.A.M.I. Elmessiry, *Nature* 281 (1979) 553.



Oussama Moutanabbir received the Ph.D. degree in energy and materials sciences from INRS Energy-Materials-Telecom., University of Quebec (Varenes, Canada) in 2005. His Ph.D. work was concerned with the isotope effects in ion-induced silicon layer transfer at the sub-100 nm scale. From January 2005 to December 2006, he worked as a visiting researcher and fellow of the Japan Society for the Promotion of Science at department of Applied Physics and Physico-Informatics, Keio

University (Yokohama, Japan). He worked on isotopically enriched group IV molecular beam epitaxy. In December 2006, he joined Max Planck Institute of Microstructure Physics (Halle, Germany). His research interests include isotopically engineered semiconductor low dimensional systems, wafer bonding, heterointegration of

materials, and defect in semiconductors. Since April 2009 he holds a joint appointment as a guest scientist at Nanophotonics Laboratory, RIKEN Institute of Advanced science (Saitama, Japan).



Stephan Senz received his Diploma in Physics in 1986 from Albert Ludwigs University, Freiburg, Germany, and in 1992 got his Ph.D. from the same University. Since 1993 he was postdoc at Max Planck Institute of Microstructure Physics in Halle, and later on became staff member of this institute. His fields of interest are solid state reactions on the nanometer scale, thin film growth, wafer bonding and layer transfer, nanowire and nanotube growth, X-ray diffraction and transmission electron microscopy.



Zhang Zhang is a Ph.D. student at Max Planck Institute of Microstructure Physics, Halle, Germany. He got his M.S. degree in 2007 from Department of Optical Science and Engineering, Fudan University (Shanghai, China) and his B.S. degree in 2004 from Department of physics, Sun Yat-Sen University (Guangzhou, China). His research interests include semiconductor nanowires and ordered porous materials.



Ulrich Gösele is Director of the Experimental Department II of Max Planck Institute of Microstructure Physics, Halle, Germany, and Honorary Professor of Experimental Physics at Martin Luther University Halle-Wittenberg, Germany. Staying with Max Planck Institute of Metal Physics, Stuttgart, Germany, he received his Ph.D. from the University of Stuttgart in 1975, and then worked in research laboratories of Siemens (Munich, Germany), IBM (Yorktown Heights, New York, USA), and NTT (Japan), as well as at a nuclear research center in South Africa. In 1985 he became Full Professor of Materials Science at Duke University, Durham, USA. Since 1993 he is Member of the Max Planck Society and Director at its Microstructure Physics institute in Halle. Ulrich Gösele is Fellow of the American Physical Society and the British Institute of Physics. He is a member of the German National Academy of Science. His research interests, among others, include diffusion mechanisms in solids, semiconductor wafer bonding, semiconductor nanowires, photonic crystals, ordered macro- and microporous materials, and complex oxide functional materials.